ISSN 1392–1320 MATERIALS SCIENCE (MEDŽIAGOTYRA). Vol. 22, No. 4. 2016

Effect of Carbon in Enhancing Wear Resistance of Atomized Ferrous Compact by Steam Treatment

Philomen-D-AnandRaj PERIANAYAGAM [1] *, Palaniradja KICHENARADJAO [2], GopalaKrishna ALLURU [3]

[1] *Department of Mechanical Engineering, Jawaharlal Nehru Technological University, Kakinada, India*
[2] *Department of Mechanical Engineering, Pondicherry Engineering College, Pondicherry, India*
[3] *Department of Mechanical Engineering, Jawaharlal Nehru Technological University, Kakinada, India*

crossref http://dx.doi.org/10.5755/j01.ms.22.4.13095

Received 12 September 2015; accepted 06 January 2016

Powder metallurgy compact of the composition Fe-C-Cu were prepared by compacting, sintering and steam treatment. Studies on surface morphology through Field Emission Scanning Electron Microscope (FESEM) equipped with Energy Dispersive Spectrometer (EDS), micro hardness by Vickers method and wear by pin-on-disk method for the steam treated specimen were reported. Characterization studies were done by Field Emission Scanning Electron Microscope, Energy Dispersive Spectrometer and X-Ray Diffraction analysis. The result showed that the tribological properties of the steam treated specimen were greatly influenced by its % carbon, morphology, micro hardness and iron oxide content in the steam coatings.

Keywords: powder metallurgy, sintering, steam treatment, wear rate, micro hardness, XRD.

1. INTRODUCTION

Powder metallurgy is known to be the unique method for manufacturing several components [1]. Huge information regarding the mechanical properties is available for sintered steels, but this information does not aide in studying the wear behavior of such components. This is because wear behavior is not an intrinsic property; rather it depends on the total parameters of the engineering system [2]. Varied approaches to develop and improve properties of sintered materials have been tried and proved, such as adding alloy elements, improved process parameter control, composite structure generations through hard face incorporation and finally surface modifications [3, 4].

Information and references are available in large numbers with respect to sliding wear of powder sintered iron and steel components. Dry sliding high density improved control of compaction pressure and sintering temperature resulted in lower wear rate [5 – 7]. Also alloying of phosphorus and graphite showed reduction in wear rates [5, 7 – 9]. Investigations regarding the possibility for further microstructure change on the as-sintered steels using heat treatment were also carried out [10 – 12].

During assessment has been noticed in samples of low density sintered iron, the open surface pores function as sites for both generation and subsequent collection of worn debris [13, 14]. Porosity has a complex influence on the wear behavior and it is found that an optimum porosity level showed best dry sliding wear behavior [15]. On the other hand, during fretting wear it is seen that high porous samples were prone to more oxidation and retaining the formed oxides. However, increase in applied load and amplitude brought about severe wear, in contrast to low sliding speeds wherein wear was much lesser in comparison with solid material [16].

Investigation of transitional wear behavior has been carried out by two alternatives, increasing the load at a constant sliding speed [5, 9, 17] or increasing the speed keeping the load constant [8, 18, 19]. The results observed show low wear rate at low loads since mild wear occurs with surface oxidation. At increased loads higher metallic wear is observed along with the high wear rate. The fundamental reason of wear is oxidation and oxides thus formed have been influenced by the temperature generated during the rubbing process [8, 13, 18 – 21]. Powder sintered components seem to have the advantage of holding the lubricant in the pores which help in reducing the wear in comparison to solid materials, where externally added lubricant gets exhausted [5, 7, 10, 22].

Surface treatment of sintered parts using steam treatment oxidation is a widely applied technique and such treated parts have been studied for their tribological characteristics. Determination of wear rate with respect to steam treated and untreated sintered iron at a combination of certain sliding speed/load in an inert atmosphere shows lower wear rate in steam treated sintered product [20]. Although oxide layer seems to have positive effect, yet it leads to a decrease in abrasive wear which in turn decreases the tendency to seizure [22]. As long as the oxide layer covers the surface, the rate of wear is lesser independent of chemical composition of the base material. The time the oxide layer is removed different wear mechanisms begin to operate on the surface depending on the combination of load / speed [23].

The study of friction curve helps in understanding the concept of durability distance for steam oxidation. This distance indicates where the oxide debris begins to generate which is indicated by the first fluctuation in the friction curve. Durability distance is influenced by the characteristics of the steam oxidized layer, which in turn is

* Corresponding author. Tel.: +91-9894927070.
E-mail address: *philomen@rediffmail.com* (P. Perianayagam)

influenced by the microstructure of the base material [24]. The durability distance concept has been thoroughly examined and studied using electrical contact resistance measurement. This helps in getting the effects of compaction pressure, powder grade, microstructure, oxide content and hardness with respect to wear [25].

Very few works have been reported about the surface morphology and wear characteristics specially during dry sliding for atomized premix ferrous powder with variation in carbon content in steam treated alloy conditions for shock absorber applications. This study aims at exploring the process of steam treatment and also to study the effect of carbon additions on the surface morphology, and wear behavior of the steam treated specimen.

2. EXPERIMENTAL DETAILS

2.1. Materials and methods

The following composition was obtained by mixing atomized iron powder 97 %, carbon 0.2 % and 0.8 %, copper 2 % along with 0.8 % zinc stearate which was used as a lubricant. When the percentage of carbon was increased to more than 1 % the compact became brittle, high hardness and shrinkage in growth during sintering and low hardness, negligible growth in case of less than 0.1 %. A green compact with a diameter of 25.35 mm and 7 mm thick set in a tool withdrawal type of floating die was obtained as test samples as per the ASTM standard [26] with atomized premix ferrous powders, pressed at 350 – 370 MPa, which were sintered at a temperature of 1130 °C in the presence of nitrogen in an Abbot mesh belt furnace and later cooled to 85 – 60 °C for about 35 minutes. Then for 95 minutes, steam treatment was carried out at 540 °C in an industrial furnace and then the samples were directly brought down to room temperature. Steam treatment was performed according to the ASTM Standard [27]. Sintered and steam treated specimen density was determined by water immersion as per Archimedes method [28].

2.2. Microstructure characterization

The samples were etched with 2 % Nital (98 cm^3 ethanol & 2 cm^3 nitric acid) and the microstructure was observed through an optical microscope (Leica DM 2500M) for steam treated samples. Elemental composition and worn surfaces of the steam treated disk materials was performed in a Field Emission Scanning Electron Microscope (Carl Zeiss microscopy Ltd, UK & SIGMA) equipped with energy dispersive X-ray detector. The phase structure of the steam treated coating was studied by X-ray diffraction (XRD) employing Cu Kα radiation (XPERT-3). The scanning angle (2θ) ranged from 10 to 90° with a step size of 0.026°.

2.3. Hardness and wear

Micro Hardness equipment (Matsuzawa MMT-X7 B type, Japan) as per the ASTM standard [29] was used to measure hardness at a load of HV1 and holding time of 15 s. Three micro hardness measurements were conducted and the averages of micro hardness values for the specimens with 6.0 – 6.6 g/cc in as-sintered and steam treated was reported. The wear behavior of the steam treated samples was evaluated in a computerized pin on disk wear testing machine as per ASTM G99-95 [30]. Dry sliding wear tests were performed at room temperature, under various loads (20, 40, and 60 N) with a constant sliding velocity of 0.26 m/s and a distance of 314 m. EN 31 spherical balls with a Rockwell-C hardness of 60 and 10 mm diameter were used as the counter friction pair for disks prepared with 25.35 mm diameter and 7 mm thickness at a density of 6.6 g/cc. By dividing wear volume by wear distance, the wear rate (W_r) is calculated.

3. RESULTS AND DISCUSSION

3.1. Surface morphology

Fig. 1 presents the microstructure of atomized premix ferrous powder in steam treated respectively of 0.2 % and 0.8 % of carbon, compacted to densities of approx. 6.6 g/cc, and sintered at 1130 °C. In the material with 0.2 wt.% carbon, the structure is almost ferrite microstructure. The presence of free copper is low with ferrite at the grain boundaries due to two different stages of sintering process i.e. local bonding between adjacent particles and pore rounding and pore shrinkage. High sintering temperature produces a significant improvement in the diffusion, which increases dramatically accelerate the atomic motion between particles (better sintering necks), improve the surface reduction of the particles (activate sintering), increase the sintered density, improve the homogenization, better mechanical properties and improve the porosity (rounded and closed).

Microstructure of powder with 0.8 % C, the structure is mostly pearlite, and the lamellar structure is seen in Fig.1 b. The ferrite phase is better resolved with globular pearlite in the ferrite. The pores are more affected by the reaction of the iron oxide formation, which formed at the grain boundaries of pearlite. The filled pores with oxide film formed at the grain boundaries would increase the hardness of the compact considerably. Both complete diffusion of copper and carbon into the iron matrix. The carbon diffuses readily into iron within five minutes at a temperature of 1040 °C and is known as carbon diffusion zone. Copper becomes a liquid at 1086 °C and settles at the grain boundaries, but does not penetrate the iron in the same manner as the carbon and is known as fusion zone. These findings are well agreed with earlier studies [31, 32].

The FESEM micrograph of steam treated specimens is shown in Fig. 2. It can be seen that pores that are created during compacting of the powders to a certain extent. Some pores are partially fused by sintering. The grains, which are in close proximity have partially undergone fusion and the grains far apart have formed the pores. The as-sintered material was the base for the surface treatment of steam oxidation, so that the oxides fuse interior to the pores either completely or partially.

3.2. EDS analysis of the steam treatment

The composition of the deposited steam coatings was determined using FESEM fitted with EDS detector. The weight percentage of major elements, iron oxide, carbon, copper and zinc are shown in Fig. 3.

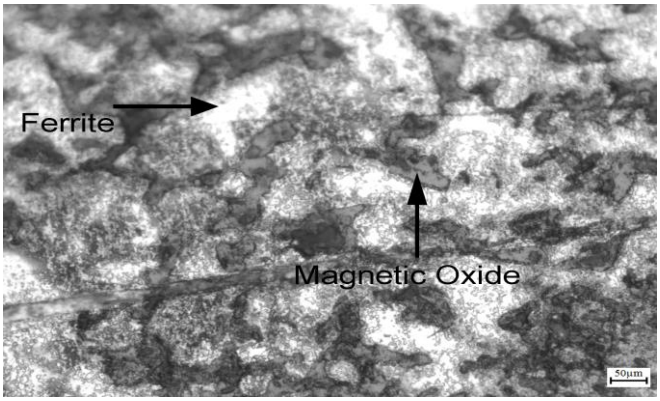

a

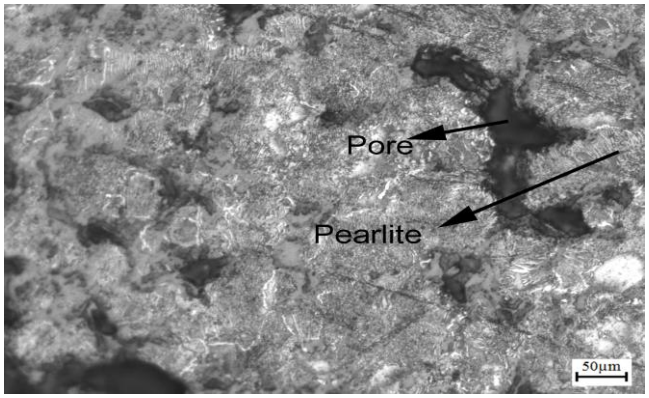

b

Fig. 1. Microstructures of atomized iron: a – 0.2 % C; b – 0.8 % C

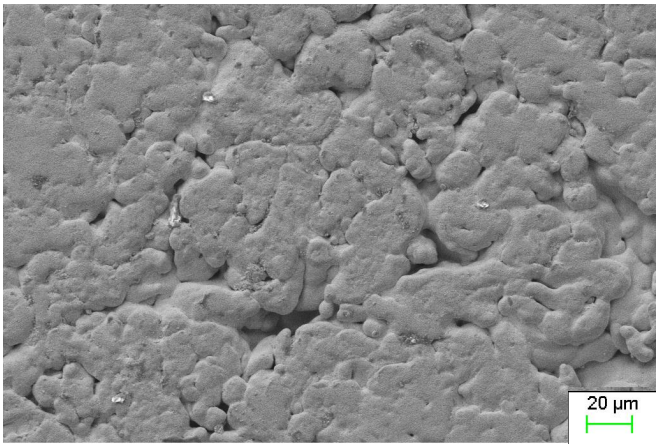

a

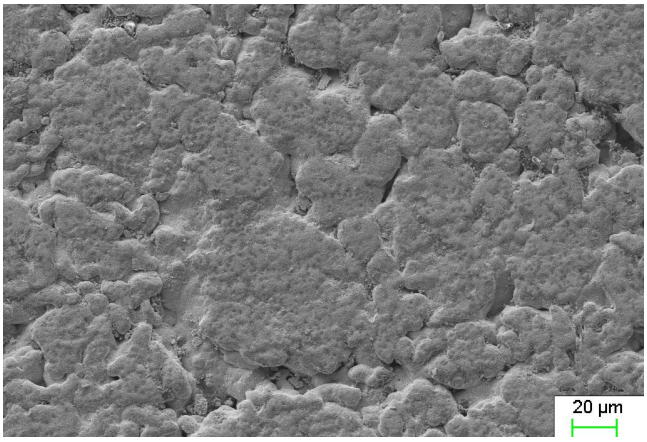

b

Fig. 2. FESEM of atomized iron: a – 0.2 % C; b – 0.8 % C

The maximum percentage of iron oxide present is the 0.2 % carbon as 97.87 wt.%.EDS analysis of 0.8 % carbon with 96.04 wt.% is shown in Fig. 4. In the EDS data (Fig. 3 and Fig. 4) suggests the presence of magnetite and hematite in the structure. Mazahery et al have reported that ferrous materials have shown the presence of oxides, which is an implication of oxide wear mechanism [33]. In the current study, high concentrations of iron oxides are observed from the EDS analysis of the steam treatment as reported by Mazahery et al. This suggests that iron oxides formation takes place through oxidizing reaction.

3.3. XRD Analysis of phases

To monitor magnetite (Fe_3O_4), hematite (Fe_2O_3) and iron (Fe) content, X-ray diffraction method has been found to be most effective and accurate. The phases present in the steam treated specimens with 0.2 % and 0.8 % carbon are shown in Fig. 5 and Fig. 6. XRD analysis shows the formed oxide layer which consists of magnetite (Fe_3O_4), Hematite (Fe_2O_3) and substrate iron (Fe). Fig. 1 show that the oxide layer covers the irregular surface and has a uniform thickness around 6 µm. The particles are loosely packed; it is observed that there is more room for steam penetration through the numerous inter-connected pores. In such cases, a great amount of (Fe_3O_4) oxide forms a layer on the surface of these pores either completely or partially filling or that helps in the prevention of plastic deformation and indentation, when the wear and hardness of these particles are tested. The formation of predominant iron oxides peak in steam treated sintered specimen was previously reported in several publications [34]. The magnetite is deposited on the surface of the parts by the following reactions:

$$3Fe + 4H_2O \rightarrow Fe_3O_4 + 4H_2. \quad (1)$$

The water vapor in the steam begins to react with iron and forms magnetite (Fe_3O_4), after being steam treated for 1 hour at a temperature close to but below 550 °C. The magnetite thus produced are blue grey in color, adhere strongly, have high wear resistance, and form a layer on the surface of the sample parts and inside the pores, thus forming a barrier, stopping contaminants from entering the inner structure. This proves that steam treatment enables longer shelf life of the parts than the as-sintered parts. The hydrogen liberated from the above reaction constantly dilutes the steam. If the hydrogen concentration in the steam over the surface of the specimens increases more, the above reaction is reverted and the formation of the magnetite layer is reduced. Neither the steam temperature nor the temperature of the specimens exceed 550 °C a small amount of (FeO) (Wustite) gray, flaky and loosely adhering, layer forms on all exposed surfaces of the compact according to the equation:

$$Fe + H_2O \rightarrow FeO + H_2. \quad (2)$$

When the steam temperature is below 550 °C, the temperature will condense and a hydroxide of iron will be formed according to the equation:

$$2Fe(OH)_3 \rightarrow Fe_2O_3 + 3H_2O. \quad (3)$$

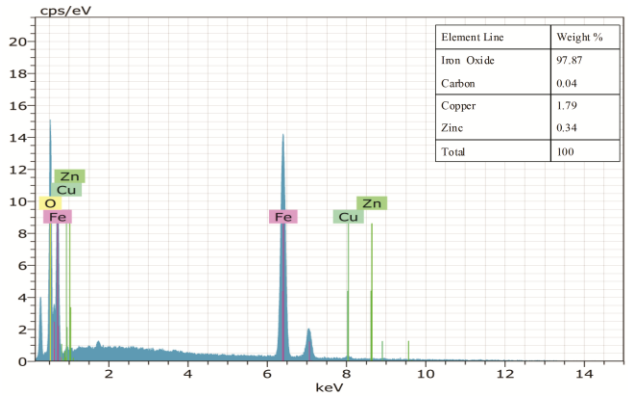

Fig. 3. EDS and composition of the 0.2 % C steam deposits

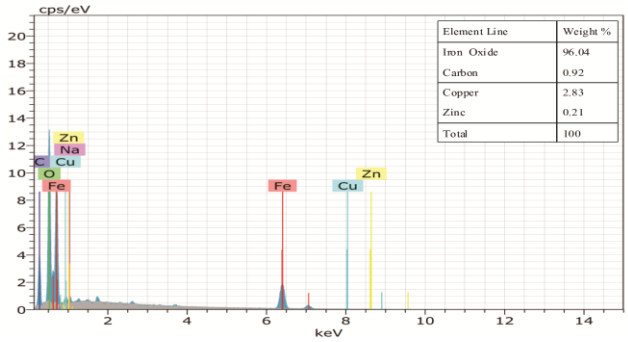

Fig. 4. EDS and composition of the 0.8 % C steam deposits

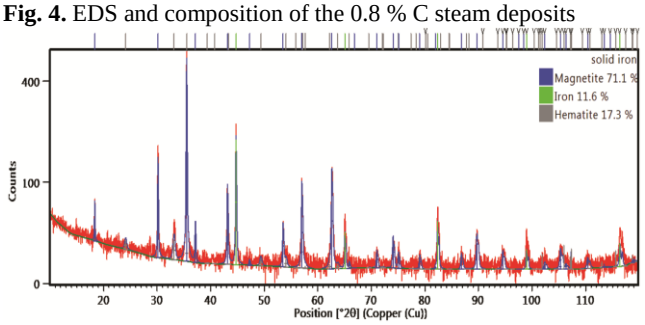

Fig. 5. X-ray diffraction peaks for 0.2 % C steam deposits

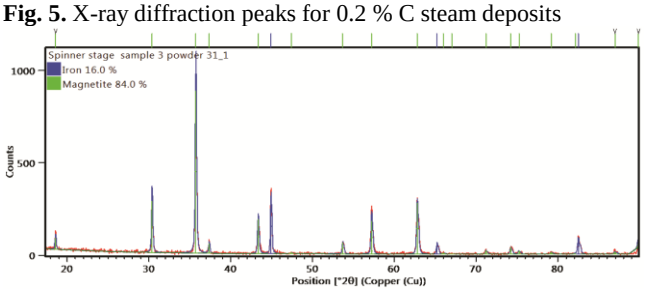

Fig. 6. X-ray diffraction peaks for 0.8 % C steam deposits

Air must be absent at all times from the furnace once heated above 320 °C. If the present air causes the parts to exhibit non-uniform color, then the oxide may form a small amount of (Fe_2O_3) (Hematite).

3.4. Hardness, wear analysis

Fig. 7 shows the effect of compacting pressure and carbon content on the hardness of as-sintered and steam treated components. The high hardness of Fe-Cu-C components in as-sintered condition is mainly due to the combined effect of copper causing precipitation strengthening. The steam treated specimens have considerably higher hardness compared to as-sintered specimens with increasing compaction pressure and carbon content. As the amount of pearlite that contains the carbon increases, hardness increases correspondingly until a carbon content of 0.8 %, at which point the structure consists entirely of pearlite (Fig. 1 b). At 0.2 % carbon, ferrite forms at the grain boundaries (Fig. 1 a), which reduces the hardness.

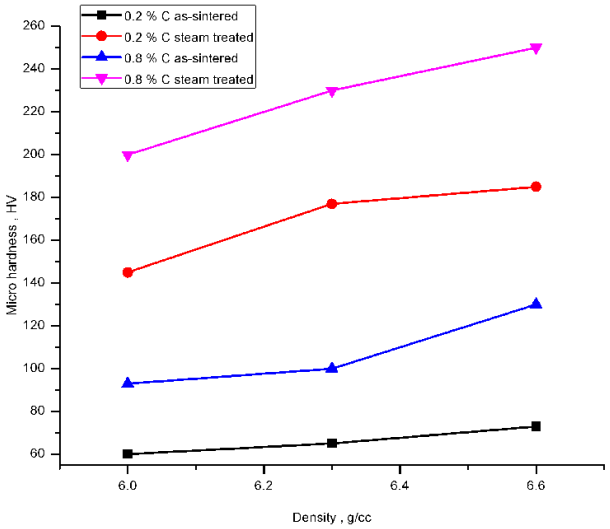

Fig. 7. Influence of carbon content upon the properties of steam treated iron

Another significant observation is that steam oxidation effectively increases the hardness when sintered density is increased. The increase in hardness in Fe-Cu-C coatings is mainly due to the formation of the magnetite during the steam treatment as determined from XRD studies as shown in Fig. 5 and Fig. 6.

Fig. 8 shows clearly that the friction co-efficient (FC) of the 0.2 % carbon at a stable load of 60 N of 6.6 g/cc kept increasing and decreasing and later stabilized at around 0.429 and Fig. 9 shows the increase and decrease of friction co-efficient of 0.8 % carbon which later stabilized at 0.617. 0.2 % carbon curve is divided into the following four stages as shown in Fig. 8 as stage 1: initial sharp increase, stage 2: gradual increase, stage 3: secondary sharp increase and stage 4: surface with nearly constant value.

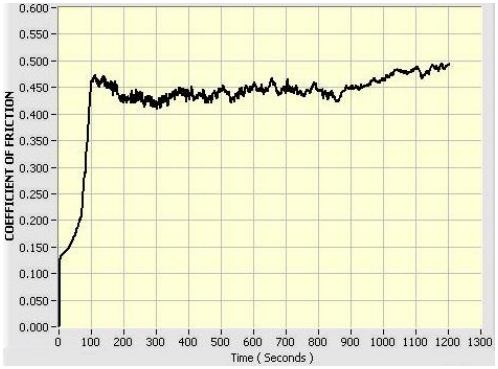

Fig. 8. Friction coefficient profile of 0.2 % C steam coating

On the other hand, in 0.8 % carbon components, the stages 2 and 3 are missing which means coefficient of friction increases directly from the initial stage to reach the final surface values without going through the intermediate stages 2 and 3 as shown in Fig. 9. The wear and tear rate of 0.2 % and 0.8 % carbon steam treated materials are shown in Fig. 10. It was also noted that the rate of wear decreased with increase in the level of load for each condition. Reduced wear rates were obtained when 0.8 % of carbon

after steam treatment process compared to 0.2 % of carbon. The variation is more dominant with the increased content of carbon in the steam treated specimens.

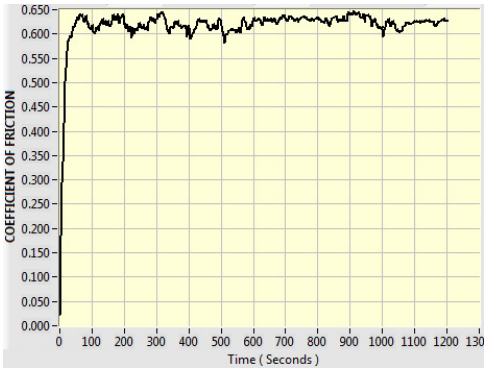

Fig. 9. Friction coefficient profile of 0.8 % C steam coating

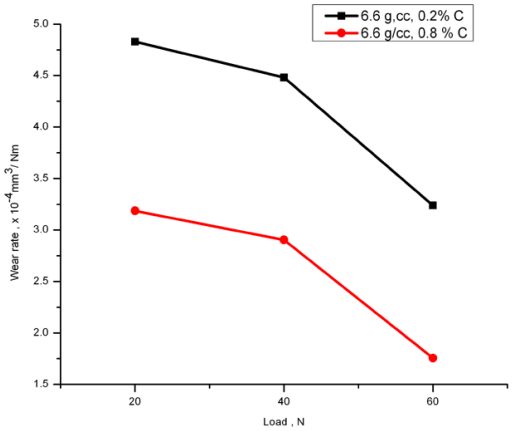

Fig. 10. Variation of wear resistance of steam coatings with respect to different % carbon

This trend is in agreement with the work of others [9, 17, 35 – 37]. In steam treated samples, hardness is one of the most important factors in case of wear and therefore wear is inversely proportional to hardness. According to [38] porosity reduces mechanical and wear strength properties.

So the author recommends surface heat treatments to improve the wear strength. This proves that the hardness of the given material played a significant role in the wear behavior. The drastic reduction in wear rate of 0.8 % carbon samples than 0.2 % carbon samples can be justified by the following reasons:

1. In this process iron oxide coatings form on the outer surface of the sample and steam diffusing through the pores effects an internal oxide coating.
2. This shows that increase in hardness during steam treatment has a relation to precipitation and oxidation. Each part will gain weight during the steam operation due to iron oxide build up in the porous powder metal.

Fig. 11 shows the wear of the 0.8 % C and the 0.2 % C in the steam treated condition. Fig. 11 a shows the presence of surface oxidation on the worn surfaces in the sliding direction [39]. Fig. 11 b shows the deformed layers with severe plastic deformation [40, 41] which indicates high metallic wear. The worn out fragments fill the pores on the disk surface and forms a protective layer as sliding advances. Since the hardness for the 0.8 % carbon steam treated is more than 0.2 % carbon steam treated samples, there is a smaller contact area which results in preventing direct metallic contact, thereby minimizing the wear rates.

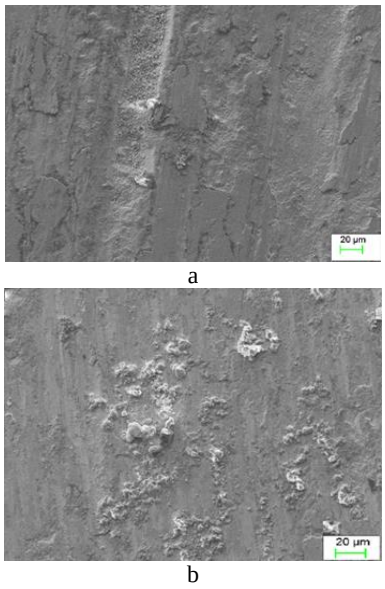

Fig. 11. Worn surfaces of atomized iron: a – 0.8 % C; b – 0.2 % C

4. CONCLUSIONS

1. Microstructure of 0.2 % carbon consisted of ferrite and pearlite and 0.8 % carbon the structure is mostly pearlite.
2. Addition of carbon and copper provides liquid-phase sintering increasing strength of the sintered components.
3. Higher hardness and wear resistance results were obtained for 0.8 % carbon steam treated PM compacts compared to the results of 0.2 % carbon steam treated compacts.
4. XRD analysis showed the developed oxide layer consists of magnetite with traces of hematite and substrate iron.
5. Oxidation and plastic deformation was found to be the dominant wear mechanism for the Fe-C-Cu based alloy in the steam treated condition.
6. Steam treatment improves the wear resistance of sintered Fe-C-Cu alloy.

REFERENCES

1. **Narasimhan, K.S.** Sintering of Powder Mixtures and the Growth of Ferrous Powder Metallurgy *Materials Chemistry and Physics* 67 2001: pp. 56 – 65.
2. **Grimanelis, D., Eyre, T.S.** Wear Characteristics of a Diffusion Bonded Sintered Steel with Short Term Surface Treatments *Wear* 262 2007: pp. 93 – 103.
3. **Cavdar, U., Unlu, B.S., Pinar, A.M., Atik, E.** Mechanical Properties of Heat Treated Iron Based Compacts *Materials and Design* 65 2015: pp. 312 – 317.
4. **Bell, T.** Surface Treatment and Coating of PM Components *Powder Metallurgy* 34 (4) 1991: pp. 253 – 258. http://dx.doi.org/10.1179/pom.1991.34.4.253
5. **Eyre, T.S., Walker, R.K.** Wear of Sintered Metals *Powder Metallurgy* 1 1976: pp. 22 – 30. http://dx.doi.org/10.1179/pom.1976.19.1.22

6. **Leheup, E.R., Zhang, D., Moon, J.R.** The Effect of Density on Fretting Wear of Sintered Iron *Wear* 176 1994: pp. 111 – 119.
7. **Wang, J., He, Y., Danninger, H.** Influence of Porosity on the sliding Wear Behavior of Sintered Fe-1.5Mo-0.7C Steels *Journal of Materials Engineering and Performance* 12 2003: pp. 339 – 344. http://dx.doi.org/10.1361/105994903770343204
8. **Gopinath, K.** The Influence of Speed on The Wear of Sintered Iron Based Materials *Wear* 71 1981: pp. 161 – 178.
9. **Victoria-Hernandez, J., Hernandez-Silva, D., Vite-Torres, M.** Microstructural Characterization and Sliding Wear Behavior of Ultra High Carbon Steels Processed by Mechanical Alloying *Wear* 267 2009: pp. 340 – 344.
10. **Pavanati, H.C., Straffelini, G., Maliska, A.M., Klein, A.N.** Dry Sliding of Plasma-Sintered Iron-The Influence of Nitriding on Wear Resistance *Wear* 265 2008: pp. 301 – 310.
11. **Wang, J., Danninger, H.** Dry Sliding Wear Behavior of Molybdenum Alloyed Sintered Steels *Wear* 222 1998: pp. 49 – 56.
12. **Rivolta, B., Gerosa, R., Silva, G., Tavasci, T., Engstrom, U.** Wear performance of Surface Hardened PM Steel from Pre-Alloyed Powder *Wear* 289 2012: pp. 160 – 167.
13. **Lim, S.C., Isaacs, D.C., McClean, R.H., Brunton, J.H.** The Unlubricated Wear of Sintered Steels *Tribology International* 20 (3) 1987: pp. 144 – 149. http://dx.doi.org/10.1016/0301-679X(87)90044-2
14. **Lim, S.C., Brunton, J.H.** The Unlubricated Wear of Sintered Iron *Wear* 113 1986: pp. 371 – 382.
15. **Simchi, A., Danninger, H.** Effects of Porosity on Delamination Wear Behaviour of Sintered Plain Iron *Powder Metallurgy* 47 (1) 2004: pp. 73 – 80.
16. **Leheup, E.R., Zhang, D., Moon, J.R.** Low Amplitude Reciprocating Wear of Sintered Iron *Wear* 176 1994: pp. 121 – 130.
17. **Dhanasekaran, S., Gnanamoorthy, R.** Microstructure, Strength and Tribological Behavior of Fe-C-Cu-Ni Sintered Steels Prepared with MoS_2 Addition *Journal of Material Science* 42 2007: pp. 4659 – 4666. http://dx.doi.org/10.1007/s10853-006-0385-0
18. **Gopinath, K., Rayudu, G.V.N., Narayanamurthi, R.G.** Friction and Wear of Sintered Iron *Wear* 42 1977: pp. 245 – 250.
19. **DaSilva, W.M., Binder, R., DeMello, J.D.B.** Abrasive wear of Steam-Treated Sintered Iron *Wear* 258 2005: pp. 166 – 177.
20. **Amsallem, C., Gaucher, A., Guilhot, G.** The Unlubricated Frictional Behaviour of Sintered Iron *Wear* 23 1973: pp. 97 – 112.
21. **Sudhakar, K.V., Sampathkumaran, P., Dwarakadasa, E.S.** Dry Sliding Wear in High Density Fe-2% Ni Based P/M Alloys *Wear* 242 2000: pp. 207 – 212.
22. **Dubrujeaud, B., Vardavoulias, M., Jeandin, M.** The Role of Porosity in the Dry Sliding Wear of a Sintered Ferrous Alloy *Wear* 174 1994: pp. 155 – 161.
23. **Straffelini, G., Molinari, A.** Dry sliding Behaviour of Steam Treated Sintered Iron Alloys *Wear* 159 1992: pp. 127 – 134.
24. **Molinari, A., Straffelini, G.** Surface Durability of Steam Treated Sintered Iron Alloys *Wear* 181 – 183 1995: pp. 334 – 341.
25. **DeMello, J.D.B., Hutchings, I.M.** Effect of processing Parameters on the Surface Durability of Steam-Oxidized Sintered Iron *Wear* 250 2001: pp. 435 – 448.
26. **ASTM standard B 925–03**, Standard Practices for Production and Preparation of Powder Metallurgy (P/M) Test Specimens. 2003.
27. **ASTM Standard B 935-05**, Standard Guide for Steam Treatment of Ferrous Powder Metallurgy (P/M) Materials.
28. **ASTM Standard B 311 – 93**, Standard Test Method for Density Determination for Powder metallurgy (P/M) Materials Containing Less than Two Percent Porosity 2002.
29. **ASTM Standard B 721**, Standard Test Method for Micro hardness and case Depth of Powder Metallurgy (P/M) Parts.
30. **ASTM G 99-05**, Standard Test method for Wear testing with a Pin-on-Disk Apparatus. 2010: pp. 1 – 5.
31. **RoshanKumar, D., KrishnaKumar, R., Philip, P.K.** Investigations on Dynamic Compaction of Metal Powders Part I: Experimental *Powder Metallurgy* 45 (3) 2002: pp. 219 – 226.
32. **Cias, A., Mitchell, S.C., Watts, A., Wronski, A.S.** Microstructure and Mechanical Properties of Sintered (2 – 4) Mn – (0.6 – 0.8) C Steels *Powder Metallurgy* 42 (3) 1999: pp. 227 – 233. http://dx.doi.org/10.1179/003258999665567
33. **Mazahery, A., Shabani, M.O.** Characterization of Wear Mechanisms in Sintered Fe – 1.5 wt.% Cu Alloys *Archives of Metallurgy and Materials* 57 (1) 2012: pp. 93 – 103.
34. **Molinari, A., Straffelini, G.** Wear Processes in High-Strength Sintered Alloys Under Dry Rolling-Sliding *Wear* 173 1994: pp. 121 – 128.
35. **Ji, Y.P., Wu, S.J., Xu, L.J., Li, Y., Wei, S.Z.** Effect of Carbon Contents on Dry Sliding Wear Behavior of High Vanadium High Speed Steel *Wear* 294 – 295 2012: pp. 239 – 245.
36. **Akhlaghi, F., ZareBidaki, A.** Influence of Graphite Content on The Dry Sliding and Oil Impregnated Sliding Wear Behavior of Al 2024- Graphite Composites Produced By in Situ Powder Metallurgy Method *Wears* 266 2009: pp. 37 – 45.
37. **Dhanasekaran, S., Gnanamoorthy, R.** Dry Sliding Friction and Wear Characteristics of Fe-C-Cu Alloy Containing Molybdenum Di Sulphide *Materials & Design* 28 2007: pp. 1135 – 1141.
38. **Straffelini, G., Molinari, A.** Dry Sliding Wear of Ferrous PM Materials *Powder Metallurgy* 44 (3) 2001: pp. 248 – 252. http://dx.doi.org/10.1179/003258901666419
39. **Anbuselvan, S., Ramanathan, S.** Dry Sliding Wear Behavior of As-Cast ZE41 A Magnesium Alloy *Materials and Design* 31 2010: pp. 1930 – 1936. http://dx.doi.org/10.1016/j.matdes.2009.10.054
40. **Annamalai, R., Upadhyaya, A., Agrawal, D.** An Investigation on Microwave Sintering of Fe, Fe-Cu and Fe-Cu-C Alloys *Bulletin of Materials Science* 36 (3) 2013: pp. 447 – 456. http://dx.doi.org/10.1007/s12034-013-0477-9
41. **Niranjan, K., Lakshminarayanan, P.R.** Dry Sliding Wear Behaviour of Insitu Al-TiB_2 Composites *Materials and Design* 47 2013: pp. 167 – 173. http://dx.doi.org/10.1016/j.matdes.2012.11.035